Proof Central

Please use this PDF proof to check the layout of your article. If you would like any changes to be made to the layout, you can leave instructions in the online proofing interface. First, return to the online proofing interface by clicking "Edit" at the top page, then insert a Comment in the relevant location. Making your changes directly in the online proofing interface is the quickest, easiest way to correct and submit your proof.

Please note that changes made to the article in the online proofing interface will be added to the article before publication, but are not reflected in this PDF proof.

AUTHOR QUERIES

THIS QUERY FORM MUST BE RETURNED WITH ALL PROOFS FOR CORRECTIONS

AU1) Please provide keywords for this article.

AU2) Please confirm the conflict of interest statement.

AU3) Please note that reference 57 is not cited in the text. Please cite it in the text or delete from the reference list.

AU4) Please provide the volume number and page range for reference 28.

AU5) For Figure(s) 4, The resolution of Figure[s] is too low to be used. Please provide a better quality figure[s] of 300 dpi.

PAIN®

The nucleus accumbens-prefrontal connectivity as a predictor of chronic low back pain

Adam Sunavsky[a,b], Muhammad Ali Hashmi[c], Jason William Robertson[a], Jennika Veinot[a], Javeria Ali Hashmi[a,*]

Abstract

The nucleus accumbens (NAc) and its prefrontal connections are implicated in the aetiology of chronic low back pain (CLBP). Both animal and human studies suggest that the NAc and its connections play a critical role in the transition from acute to CLBP. However, whole-brain connectivity in people with longstanding CLBP has not been systematically investigated. We used a functional connectomics approach to examine whether the 2 NAc subregions (shell and core) exhibit different whole-brain connectivity between CLBP patients and healthy controls (HCs; total N = 197). The identified connections were correlated with CLBP intensity (corrected), and their reproducibility was validated in 2 independent cohorts. These clinically relevant and reproducible connections were further leveraged to classify CLBP using machine learning. Compared with HC (n = 41), individuals with CLBP (n = 39) exhibited hyperconnectivity between the NAc shell and core and the prefrontal cortex (PFC). Although several NAc-PFC connections were linked to higher CLBP intensity, only the connections between the left NAc shell and core and the right dorsolateral PFC were reproduced in validation cohorts (total CLBP n = 53; HC n = 64). Nucleus accumbens-right dorsolateral PFC connections achieved 84% classification accuracy using logistic regression. The machine learning analyses demonstrate how knowledge-based feature selection can reliably detect CLBP. Overall, we report that NAc-PFC connectivity consistently distinguishes people with CLBP from HC and suggest an abnormal interaction between the NAc and brain regions involved in motivation, decision-making, and pain regulation.

AU1

1. Introduction

Persistent intense pain fundamentally alters the perception of noxious events, causing even harmless sensations to be perceived as painful.[47] Such alterations affect the neural pathways regulating pain and motivation, leading to avoidance behaviors and reduced activity, which further exacerbates pain.[58] The cortico–striatal pathway—critical for motivation, pain regulation, and decision-making—is believed to be a prominent feature of chronic pain.[6,26,30] Central to this circuit is the nucleus accumbens (NAc); its connections with the prefrontal cortex (PFC) have been implicated in the aetiology of chronic low back pain (CLBP).[4,25] Studies in animals and humans investigating the

transition from acute to chronic pain suggest that NAc-PFC connectivity is pivotal in CLBP development.[6,24,27,31,60] In humans, NAc connectivity with the medial PFC measured at a subacute stage of back pain predicted the persistence of back pain after 6 months to 1 year.[6] This finding was recently reproduced in an independent data set.[30] Several studies have also implicated the NAc-PFC axis in altered regulation of motivation, emotion, and sociability in human[6,21,46] and animal[24,27,60] models of chronic pain. Recently, Makary et al.[31] found that functional connectivity of the 2 main NAc substructures, the shell and core, with the rostral anterior cingulate cortex (BA 32), differentiated people with persistent back pain from those who recovered. Considering the involvement of the NAc in motivational processes, aberrant NAc connectivity begets a modulated experience of pain associated with changes in coping, motivation, attention toward pain, and emotion regulation.[2]

Nucleus accumbens connectivity has been studied for its involvement in the development of chronic pain, but its role in the symptomatology of fully developed CLBP remains ambiguous. Observing brain regions that have a synchronized pattern of fluctuations with the NAc in resting-state functional MRI(fMRI) can be a useful marker for detecting CLBP. Whole-brain functional connectivity of NAc substructures has been used to predict the transition from acute to chronic back pain, but the accumbens' role in long-standing CLBP needs systematic investigation. From animal work, it is well-known that NAc core and shell have functionally different roles, particularly in reward processing and learning, but whether these 2 subregions show differences in functional connectivity within and between CLBP and control populations is unknown.[5,31,46]

In this study, we first investigate whether the NAc exhibits significant connectivity differences between healthy individuals and those with CLBP. We analyze whole-brain resting-state functional

connectivity (rsFC) of the NAc shell and core and identify rsFC differences between groups. Subsequently, we determine functional connections that are significantly correlated with CLBP intensity to identify clinical relevant connections. We then test the reproducibility of clinically relevant rsFC patterns in 2 additional cohorts with varying demographics and MRI acquisition parameters. We deploy receiver operator characteristic curves, logistic regression, and machine learning (ML) to evaluate the accuracy of clinically relevant NAc connections in classifying healthy control (HC) and CLBP groups. We hypothesized that NAc-PFC connectivity would reliably distinguish CLBP from HC groups, and that a subset of rsFC patterns would reproduce between different study cohorts.

2. Methods

2.1. Participants

This study was approved by Nova Scotia Health Research Ethics Board. This study is part of a larger study directed at understanding biopsychosocial and neurological factors associated with treatment failure in CLBP (ClinicalTrials.gov randomized controlled trial #NCT02991625). The main goal of this project was to study the scope and limits of neuroimaging for identifying reproducible and reliable findings that can pinpoint chronic pain mechanisms. Healthy and CLBP participants were recruited through advertisements posted in the community around Dalhousie University and the Victoria General Hospital in Halifax. Chronic low back pain patients were additionally recruited from the Pain Management Unit of the Victoria General Hospital and other clinical centres in the community. Both HC and CLBP patients were required to be right-handed, between the ages of 18 and 75 years, and comfortable with reading, writing, and taking instructions in English. Subjects were excluded if they had medical conditions that would interfere with the study (eg, respiratory or cardiac conditions), contraindications to MRI scanning (eg, claustrophobia, metal implants, or dental braces), or visual impairment that could not be corrected with eyewear or contact lenses. In addition, healthy participants were excluded if they had ongoing acute pain, chronic pain, nerve compression resulting in sensory loss, or if they were taking pain medications. Chronic back pain patients were required to have had low back pain for 6 or more months and an average of at least 4/10 daily pain intensity on the Brief Pain Inventory (BPI)[13] 2 weeks before enrolment.

The data were subdivided into a test cohort (cohort 1: n = 39 CLBP and 41 HC), an in-house validation cohort (cohort 2: n = 18 CLBP, n = 31 HC), and an offsite validation cohort (cohort 3: n = 34 CLBP and 33 HC). Cohort 3 was obtained from openpain.org that used different fMRI acquisition parameters. The open pain project (Principal Investigator: A. Vania Apkarian, PhD at Northwestern University) is supported by the National Institute of Neurological Disorders and Stroke and National Institute of Drug Abuse.

2.1.1. Cohort 1

One resting-state scan from 41 HC and the average of 2 resting-state scans from 39 CLBP patients were used as the test cohort. Note that during analysis, we examined the effects of each of the 2 CLBP resting-state scans separately with the HC resting-state scan before averaging them. The significant findings were established in cohort 1 and were further tested for reproducibility in cohorts 2 and 3.

2.1.2. Cohort 2

Data from a single resting-state fMRI scan were compared between 19 CLBP patients and 31 HC participants. This data set

included the participants who had only 1 resting-state scan available, along with newly recruited participants scanned during the time of analysis for cohort 1. This in-house data set provided an opportunity to test the reproducibility of the results, using onsite data with identical acquisition parameters but varying demographic profiles. This allowed for the assessment of reproducibility across consistent imaging conditions, but different participants.

2.1.3. Cohort 3

Data consisting of 1 resting-state scan were compared between 33 HC and 34 CLBP. These offsite data were obtained from openpain.org and were used for testing reproducibility in data with different demographic and acquisition parameters.

2.2. Neuroimaging procedure

Cohorts 1 and 2 data were collected with a 3.0 T MRI scanner (Discovery MR750; General Electric Medical Systems, Waukesha, WI) with a 32-channel head coil (MR Instruments, Inc, Minneapolis, MN) at the Biomedical Translational Imaging Centre at the Veterans' Memorial Building of the Queen Elizabeth II Health Sciences Centre in Halifax, NS, Canada. To minimize movement, participants' heads were fitted with foam padding. Participants were reminded to keep their head still before each scan took place, and ear plugs were provided to reduce noise levels.

We acquired T1-weighted anatomical images (GE sequence IR-FSPGR: field of view = 224 × 224 × 184 mm; in-plane resolution = 1 × 1 × 1 mm; reptition time [TR]/echo time [TE] = 4.4/1.908 milliseconds; flip angle = 9°) from both HC and CLBP patients. Blood oxygenation level–dependent signal sequences for fMRI were acquired using a multiband EPI sequence: field of view = 216 × 216 × 153 mm; in-plane resolution = 3 × 3 × 3 mm; TR/TE = 950/30 milliseconds, SENSE factor of 2, acceleration factor of 3. Reverse phase-encoded images were also acquired to enable distortion correction. Only resting-state scans were used for these analyses: Sequences of 500 volumes were acquired from all subjects with eyes open, staring at a fixation cross displayed on a screen.

Cohort 3 (the second validation data cohort) was collected using an 8-channel head coil with parameters TR/TE = 2500/30 milliseconds and voxel size of 3.44 × 3.44 × 3.44 mm, with the scan lasting 305 volumes (762.5 seconds) for 17 CLBP patients and 17 HC; 244 volumes (610 seconds) for 17 CLBP patients and 7 HC; and 300 volumes (750 seconds) for 9 HC.

2.3. Preprocessing

All neuroimaging data were preprocessed with the Analysis of Functional NeuroImages,[14] FreeSurfer,[16] and FMRIB Software Library (FSL)[23] packages based on scripts provided by the 1000 Functional Connectome Project.[8] The parameters for preprocessing are based on previously published work.[3,29,36]

The T1 anatomical images were preprocessed using Free-Surfer's autorecon1 sequence, which includes motion correction, intensity normalization, and Talairach transformation. Masks were then generated for stripping the skull away from the image, leaving only the brain; these masks were reoriented to match the original scans then used to crop it. These skull-stripped images were retained for later use.

The functional data were then preprocessed. First, they were corrected for field map distortion using FSL's topup. Next, the first

5 volumes were discarded for signal equilibrium, then the data were corrected for motion through Fourier interpolation. At this point, 6 motion parameters were calculated for the subject's rotational movement around 3 degrees of freedom (pitch, yaw, and roll axis) and cardinal directional movement in the x-, y-, and z-planes. Then, the skull was stripped, and a sample image from the mean-aligned data was extracted for registration. After that, spatial smoothing was performed using a Gaussian kernel with a full width at half maximum of 6 mm, and the voxels were intensity-normalized, temporally filtered (0.005-0.3 Hz), and detrended. However, due to the potential concern of spatial smoothing negatively affecting spatial resolution, we also ran the same preprocessing procedure without the 6 mm smoothing filter and tested whether they produced the same results for the main study conclusions. Next, nuisance time courses for the global signal, cerebrospinal fluid, and white matter were calculated using masks from the image segmentation of the participant's T1-weighted data with a tissue-type probability threshold of 80%. These nuisance signals, along with the 6 motion parameters, were then removed by regression in the native functional space. Functional images were then registered to the Montreal Neurological Institute (MNI-152) standard template using FMRIB's Linear Image Registration Tool in 3 steps: (1) registering the native space structural image to the MNI-152 2 mm template using a 12 degree of freedom linear affine transformation; (2) registering the native space functional image to the high-resolution structural image with a 6 degree of freedom linear transformation; and (3) computing native functional to standard structural warps by concatenating the matrices computed in the first 2 steps.

2.4. Data quality

For data quality verification, we calculated maximum framewise displacement and the derivative of variability across voxels, using previously published methodologies[37] to assess and exclude participants with high motion. Participant data with maximum framewise displacement above 3 mm or derivative of variability across voxels outliers in more than 30% of the acquired data were removed from the analysis.[38] None of the participants showed motion above these thresholds.

2.5. Brain parcellation and time series extraction

We divided the brain's spatial domain into a set of nonoverlapping regions using an optimized Harvard-Oxford parcellation with 131 regions that have been previously used in our laboratory.[22,38,48] However, because our main seed regions of interest (ROIs) were the shell and core of the NAc, we replaced the bilateral NAc regions provided by the Harvard-Oxford parcellation with 4 ROIs representing the left and right shell and core from a parcellation scheme derived from diffusion tractography,[11] as they closely matched the regions demarcated by immunohistochemistry. Thus, a total of 133 regions were used in the analysis.

To make these new NAc ROIs compatible with the rest of the data set and to ensure no overlap, the original masks provided by Cartmell[11] were used as a reference to draw new masks using the edit mode in FSLeyes and the following parameters: (1) 3D voxel mode, (2) selection size = 1, (3) MNI 2 mm^3 standard space, (4) lower threshold cut-off of 0.495, and (5) upper threshold cut-off of 0.900. This resulted in ROIs with 14 voxels for the left core, 28 voxels for the right core, 43 voxels for the left shell, and 50 voxels for the right shell. The (x, y, z) coordinates for the left core were (-10.2, 14.3, -6.9), right core (11.6, 15.7, -7.4), left shell (-8.2, 9.9, -9.2), and right shell (7.5, 9.8, -8.7) in the MNI space. These

masks largely overlapped those from other studies parcellating the shell and core.[5,53,54] A depiction of the core and shell parcellation used is provided in Supplementary Figure 1 (available at http://links.lww.com/PAIN/C271).

The blood oxygen level–dependent time series from each of the 133 parcellated regions were extracted from each voxel and averaged, resulting in 133 time series for each participant. The left and right NAc shell and core time series were correlated with the remaining 129 regions to create 4 × 129 correlation matrices that described the rsFC of the NAc.

2.6. Functional connectivity analysis

Functional connectivity analyses were conducted in MATLAB (R2020a; The Mathworks, Natick, MA). Within and between group analysis were performed using a 2-way analysis of covariance (ANCOVA) with a 2 × 2 factorial design (HC/CLBP × shell/core) in the left and right sides separately with age as a covariate of no interest. Specific connections that were different in within-group (shell > core and core > shell) and between-groups (CLBP > HC and CLBP < HC) were extracted and post hoc t tests were conducted for the 4 × 129 edges with false discovery rate (FDR) correction at $q < 0.05$. Finally, age and sex effects were tested using an ANCOVA on the significant CLBP > HC analyses with age and sex as covariates of no interest in cohort 1. In addition, age and sex effects were tested by pooling the combined data from all 3 cohorts and comparing CLBP and HC by using a multivariate ANCOVA (MANCOVA). Brain images were created using BrainNet Viewer.[52] To describe the brain subnetworks involved in shell and core connectivity and their differences between HC and CLBP patients, we determined whether the significant nodes from the rsFC analysis above belonged to one of the 5 canonical resting-state networks: (1) subcortical, (2) sensory, (3) default mode, (4) attention/executive, and (5) language/memory, as described previously.[22,38]

To verify and test reproducibility of the findings, we assessed the connections in the main results from cohort 1 for their clinical relevance by analyzing the correlations between all surviving connections and CLBP intensity. After evaluating skewness and kurtosis, Pearson R correlations were performed with the connectivity measures. The connections that were significantly associated after correction for multiple comparison (FDR $q < 0.10$) were further assessed for reproducibility in the remaining cohorts.

2.7. Questionnaires

For patient characteristics, we used theBPI,[13] Beck Depression Inventory,[7] and McGill Pain Questionnaire (MPQ).[33] Participants also provided information on medications they were currently taking to manage their pain, which was quantified using the Medication Quantification Scale (MQS).[20] Pain intensity scores were evaluated by the pain intensity subscale of the Neuropathic Pain Scale.[18] In addition, we used the Pain Catastrophizing Scale, which has subscales of pain rumination, magnification, and helplessness.[45] The Pain Vigilance and Awareness Questionnaire[32] was used with subscales of attention to pain and attention to changes in pain. All questionnaires were administered through REDCap (http://www.project-redcap.org); data were stored electronically. Questionnaire responses and demographic data were compared groupwise between HC and CLBP subjects using independent-sample t tests. Equality of variances were checked with the Levene test; if any comparisons failed, then appropriately adjusted statistics were reported.

2.8. Reproducibility in additional data cohorts

To assess reproducibility of the domain knowledge-based predictors derived from NAc connectivity, we used a stepped approach. First, we tested whether the findings replicated in cohorts 2 and 3 (combined and separately) within each cohort. At this stage, we evaluated the predictive accuracy of individual features using receiver operating characteristic (ROC) curve analysis of each predictor separately. Second, we examined whether combining only reproducible features in a logistic regression model improved classification accuracy by accounting for additional variance. While ROC curves assess the discriminative power of individual features within cohorts, logistic regression evaluates predictive performance by integrating features. Third, we randomized and split data from all 3 cohorts into training and holdout test sets, reducing cohort-specific effects. We then tested whether a ML classifier trained on those domain knowledge-driven features generalized to previously unseen data. For a schematic representation of the analyses and data used for each one, please refer to Figure 1.

The first set of reproducibility analyses relies on a statistical approach to assess reproducibility across cohorts with specific demographics and characteristics The NAc-PFC connections that were significantly correlated with chronic pain intensity were assessed for reproducibility and accuracy for classifying between CLBP and HC groups in the test data set (cohort 1) and in the validation data set (cohort 2 and 3). We checked the sensitivity and specificity of the independent connections in distinguishing the HC from CLBP, and we plotted ROC curves and calculated the area under the curve (AUC) for each NAc-PFC functional connectivity in cohort 1 and in validation sets (cohorts 2 and 3). Area under the curve >0.9 was considered a good predictor, 0.7 < AUC < 0.9 was considered a moderate predictor, and AUC <0.7 was considered a weak predictor.

Second, the connections that reproduced between cohorts were further evaluated for reproducibility and accuracy using logistic regression in cohort 1 and combined cohorts 2 and 3. A logistic regression using the ENTER method was applied to the pooled data from all 3 cohorts to estimate cumulative accuracy in classifying CLBP from HC.

Third, the statistical approach was compared with a ML-based approach. For ML, we used the finalised metrics for training a ML-based classifier using data combined and randomised from cohorts 1, 2, and 3. The data set consisted of 197 samples with 4 features and a target label. The data were initially split into training and test (hold out sample) sets with an 80 to 20 split. Randomization in ML is critical because without it—if the data were split based on distinct cohorts—the model would learn to classify based on the cohort-specific features such as demographics, clinical characteristics, or scanning parameters. This would bias the model toward recognizing those specific cohort attributes rather than general patterns, resulting in poor generalizability and overfitting.[55] Hence, the final 4 rsFC metrics
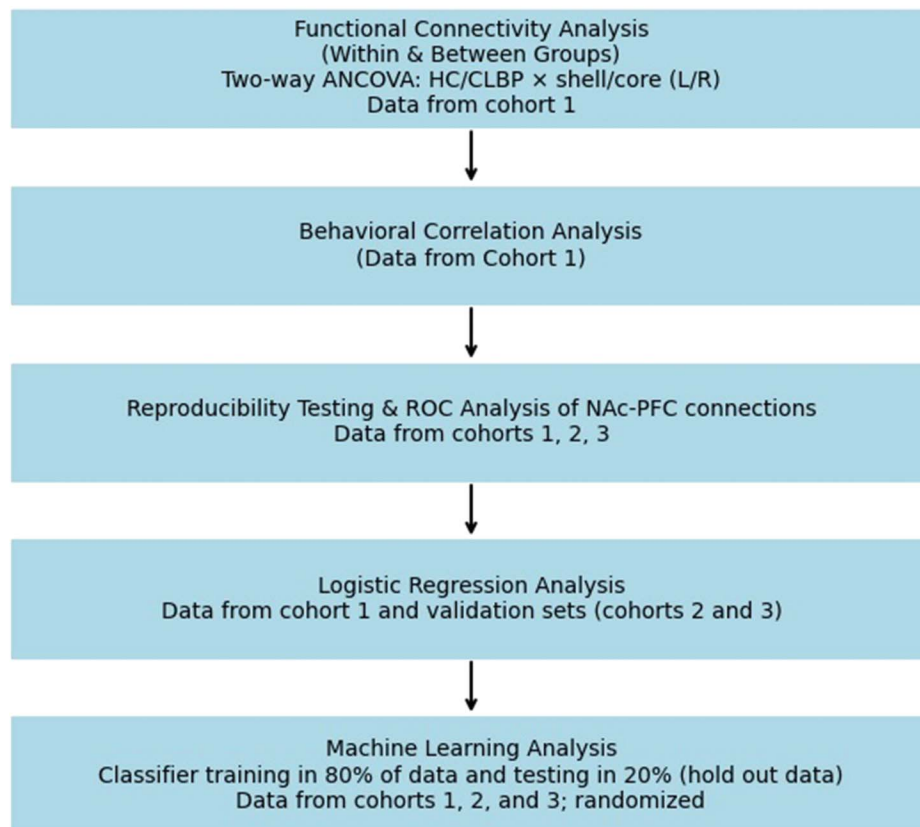
Figure 1. Schematic representation of the study analyses and data used for each analysis. ANCOVA, analysis of covariance; CLBP, chronic low back pain; HC, healthy control; NAc, nucleus accumbens; ROC, receiver operator characteristics.

for the total 197 participants were used for classifying the 2 target labels (HC n = 105 and CLBP n = 92). To evaluate the performance of various classifiers, we implemented 5-fold cross-validation for training and then tested the accuracy of the trained classifiers on the 20% of data held out.[25,38] The 4 classifiers tested were logistic regression, random forest, support vector machine, and k-nearest neighbors. Each classifier's hyperparameters were tuned using cross-validation, which optimizes the model's performance by systematically searching for the best combination of values. Accuracy and F1 score were the key performance metrics used in this study. Accuracy measures the proportion of correctly classified instances of the total instances, providing an overall effectiveness of the model; F1 score, which is the harmonic mean of precision and recall, balances false positives and false negatives. This makes it particularly useful for imbalanced data sets where class distribution is unequal.

3. Results

Participant demographics and clinical characteristics of the CLBP group are described in **Table 1**. In the initial data set (combined rest 1 and 2), CLBP patients were significantly older ($t(94)$ = 4.713, $P < 0.001$), had significantly higher depression scores ($t(91)$ = 5.806, $P < 0.001$), and had significantly higher pain catastrophizing scores ($P < 0.001$) relative to HC. In cohorts 2 and 3, there were no significant differences other than CLBP patients having higher depression scores relative to healthy participants ($P < 0.001$).

3.1. Nucleus accumbens core and shell show different patterns of connectivity with resting-state brain networks
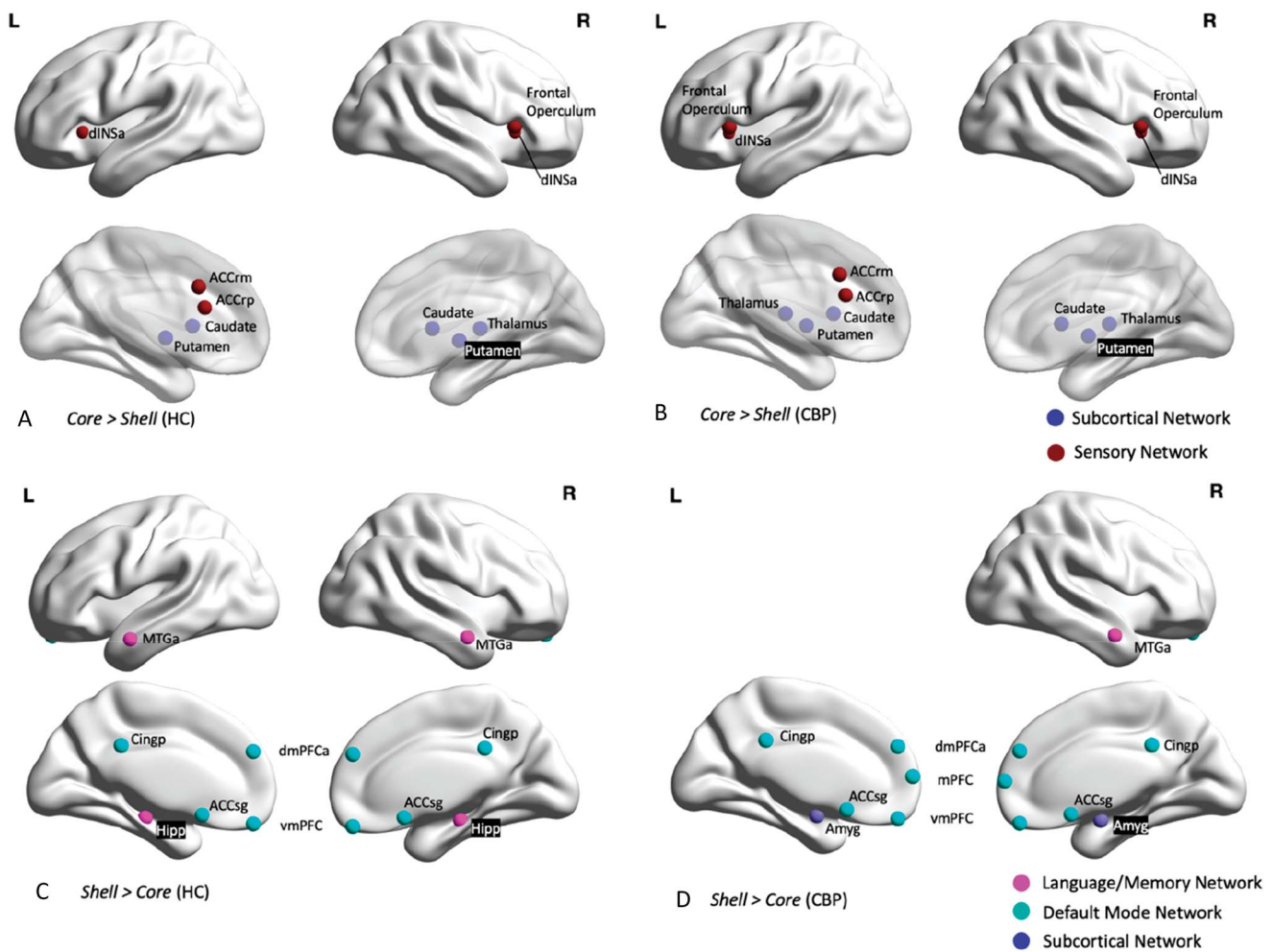
In both CLBP patients and HC, the NAc core was more synchronized with the salience network and subcortical regions (caudate, putamen, and thalamus) relative to the NAc shell (**Fig. 2**). In contrast to the NAc core, the NAc shell showed relatively greater synchrony with default mode network (DMN) regions such as the ventromedial PFC and posterior cingulate cortex, and with language/memory networks regions such as the hippocampus, middle temporal gyrus, and amygdala (whole-brain corrected at $P < 0.05$; within group analysis). Supplementary Table 1 (available at http://links.lww.com/PAIN/C271)

Table 1

Demographic and clinical parameters in the chronic low back pain and healthy control groups in the initial cohorts 1 to 3.

	No. of CLBP	No. of HC	CLBP	HC
Cohort 1: Test data set				
Age	57	41	43.02 ± 1.82	31.76 ± 1.55***
Sex	57	41	F: 39; M: 18	F: 22; M: 19
PCS	52	41	21.40 ± 1.37	12.59 ± 1.56***
BDI-II	52	41	15.42 ± 1.40	5.90 ± 0.86***
Time since diagnosis (y)	40	—	7.48 ± 0.98	—
Duration of treatment (y)	40	—	7.05 ± 0.84	—
MPQ sensory	52	—	15.90 ± 0.85	—
MPQ affective	52		4.88 ± 0.40	
NPS total	52	—	46.25 ± 1.74	—
NPS pain intensity	52	—	59.04 ± 2.82	—
BPI average pain	53	—	51.74 ± 2.12	—
MQS	54	—	6.61 ± 0.88	—
Cohort 2: Validation data set I				
Age	19	31	45.581 ± 14.01	44.83 ± 13.32
Sex	18	30	F: 14; M: 17	F: 11; M: 7
BDI-II	15	30	13.44 ± 1.81	8.03 ± 1.27***
Time since diagnosis (y)	9	—	7.96 ± 1.99	—
Duration of treatment (y)	10	—	5.88 ± 0.97	—
VAS (MPQ)	14	—	5.5 ± 0.1	—
MPQ sensory	15	—	16.44 ± 1.544	—
MPQ affective	15	—	4.63 ± 0.49	—
NPS total	15	—	46.06 ± 2.328	—
NPS pain intensity	15	—	66.25 ± 3.14	—
BPI average pain	15	—	57.5 ± 2.57	—
MQS	18	—	6.6 ± 1.6	—
Cohort 3: Validation data set II				
Age	34	33	49.24 ± 1.47	49.61 ± 1.39
Sex	34	33	F: 15 M: 19	F:14 M:19
BDI-II	34	33	6.26 ± 1.00	1.58 ± 0.46
Pain duration (y)	34	—	15.74 ± 1.94	—
VAS (MPQ)	34	—	6.66 ± 0.29	—
Combined cohorts: Average of validation data sets I and II				
Age	51	54	47.7 ± 0.2	47.5 ± 0.18
Sex	52	54	F: 27; M: 25	F: 30; M: 36
VAS (NPS/MPQ)	50	—	6.3 ± 0.03	—

Significances: *** $P < 0.001$. Age was added as a covariate of no interest in whole-brain analyses on test data sets. The validation set was matched for age.
BDI-II, Beck Depression Inventory-II; BPI, Brief Pain Inventory; CLBP, chronic back pain; F, female; HC, healthy controls; M, male; MPQ, McGill Pain Questionnaire; MQS, Medication Quantification Scale; NPS, Neuropathic Pain Scale; PCS, Pain Catastrophizing Scale; SEM, standard error of the mean; VAS, visual analog scale.

Figure 2. Functional connectivity contrast analyses show differences in connectivity of the NAc core and shell *within* HCs and CLBP patients. (A) The significant core > shell contrasts in HC and (B) in CLBP patients. Overall, the core was more connected to subcortical and sensory network regions in both groups. (C) The significant shell > core contrasts in HC and (D) in CLBP patients. These show more connections to language, memory, and default mode network regions in the shell relative to the core in both groups. For the complete list, see Supplementary Table 1 (available at http://links.lww.com/PAIN/C271). Left and right brain images represent sagittal views; the top set are viewed from the lateral side while the bottom set are viewed from the medial side at the midbrain. Whole-brain corrected at $P < 0.05$. ACCrm, rostral anterior cingulate cortex mid posterior; ACCrp, rostral anterior cingulate cortex posterior; ACCsg, subgenual anterior cingulate cortex; Amyg, amygdala; CLBP, chronic back pain; Cingp, cingulate gyrus posterior division; dINSa, dorsal anterior insula; dmPFCa, dorsal medial prefrontal cortex anterior division; HC, healthy control; Hipp, hippocampus; mPFC, medial prefrontal cortex; MTGa, middle temporal gyrus anterior division; vmPFC, ventromedial prefrontal cortex.

provides a comprehensive list of all the significant edges found for each contrast in HC and CLBP.

3.2. Differences in nucleus accumbens connectivity between people with chronic back pain relative to healthy controls

First, we observed that there was no significant difference between shell and core connectivity in the region-wise (main effect of region, shell × core in the right [$P = 0.635$] or left [$P = 0.994$] side). On testing group differences, there were significant differences between CLBP and HC in NAc whole-brain connectivity in the left ($P = 0.003$) and right ($P = 0.003$) NAc (main effect of group, corrected for age and sex, and for multiple comparisons at $q < 0.05$, between-group analysis). Participants with CLBP demonstrated significantly more connectivity between NAc and several prefrontal regions including the dorsolateral (dlPFC) and dorsomedial PFC (dmPFC) relative to the healthy group (**Fig. 3**; **Table 2**). In addition, CLBP patients demonstrated hypoconnectivity with sensory regions and language memory networks.

3.3. Associations between resting-state functional connectivity networks, pain intensity, catastrophizing, and hypervigilance

The identified NAc-PFC connections were correlated with clinical symptoms of CLBP. Chronic pain intensity was associated with NAc-PFC connections (**Fig. 4**, FDR $q < 0.10$ for each NAc node) showing that higher pain intensity was correlated with high connectivity in the left NAc shell-right dlPFC ($r = 0.32$, $P = 0.022$), left NAc core-right dlPFC ($r = 0.37$, $P = 0.007$), left shell-left dmPFCa ($r = 0.33$, $P = 0.018$), left shell-right dmPFCa ($r = 0.37$, $P = 0.007$), left core-left dmPFCa ($r = 0.36$, $P = 0.010$), and the left core-right dmPFCa ($r = 0.43$, $P = 0.001$). Finally, in the CLBP < HC contrast, chronic pain intensity was significantly negatively correlated with the left core-right temporal occipital fusiform cortex ($r = -0.50$, $P < 0.001$).

Next, the connectivity measures that correlated with pain were also explored for their correlation with pain catastrophizing and hypervigilance (exploratory uncorrected result). There was a significant association between hypervigilance to changes in pain and rsFC between the left and right NAc shell and the left
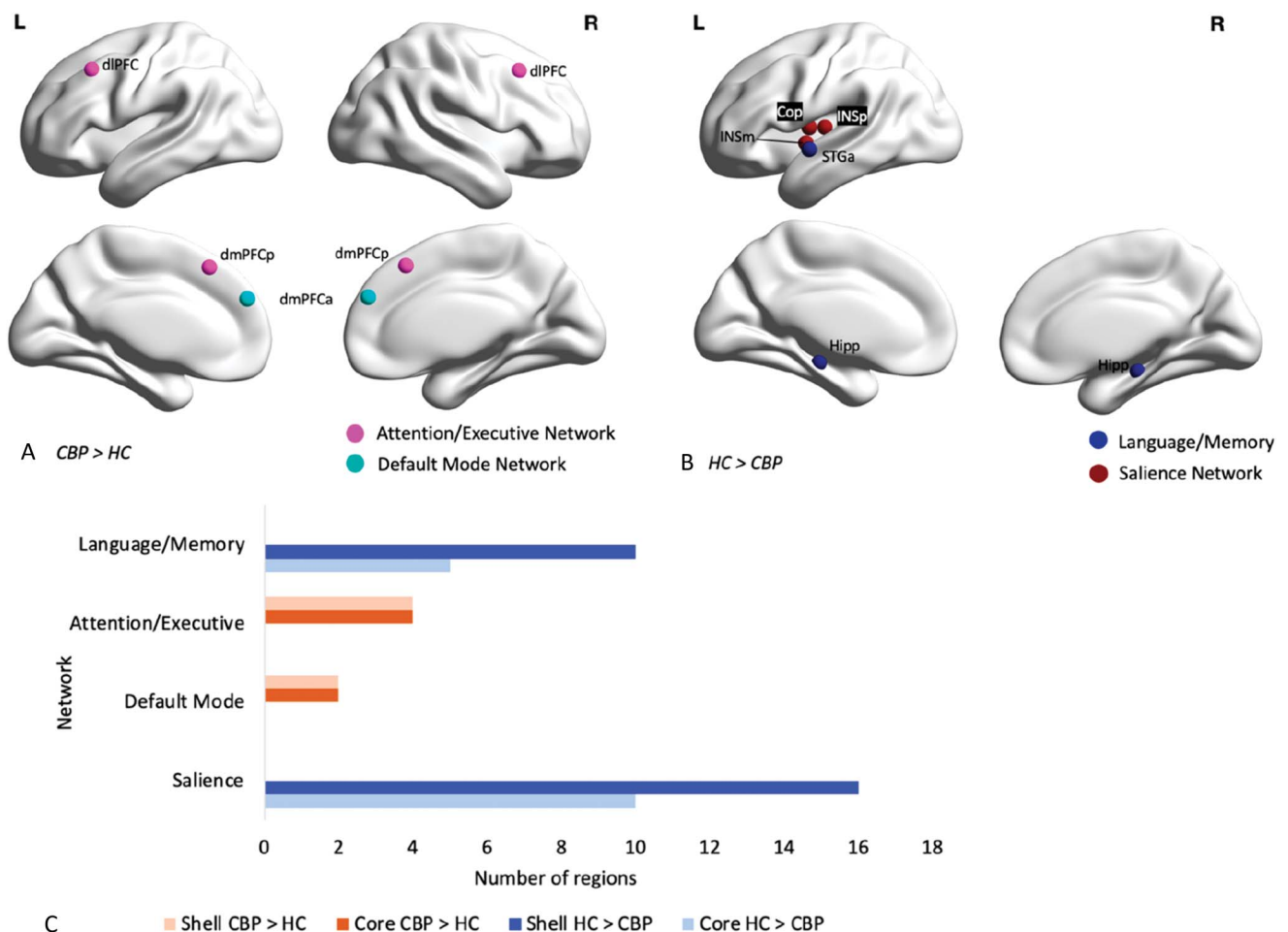
Figure 3. Functional connectivity contrast analyses revealed connectivity differences between HCs and CLBP patients in both the NAc shell and core. (A) The significant CLBP > HC contrasts. (B) A sample of the significant HC > CLBP nodes. (C) Quantification of significant nodes in the CLBP > HC and HC > CLBP contrasts into their respective networks. CLBP patients had more connections to the attention/executive and default mode networks, while HC had more connections to language/memory and salience sensory networks. Left and right brain images represent sagittal views; the top set are viewed from the lateral side, while the bottom set are viewed from the medial side at the midbrain. Whole-brain corrected at $P < 0.05$. CLBP, chronic back pain; Cop, central operculum; HC, healthy control; INSm, middle insula; INSp, posterior insula; dlPFC, dorsolateral prefrontal cortex; dmPFCa, dorsal medial prefrontal cortex anterior division; dmPFCp, dorsal medial prefrontal cortex posterior division; Hipp, hippocampus; STGa, superior temporal gyrus, anterior division.

dmPFCa ($r = 0.28$, $P = 0.039$) and the left dlPFC ($r = 0.33$, $P = 0.022$), respectively. Moreover, pain catastrophizing scores were significantly correlated with the left shell ($r = 0.34$, $P = 0.014$) and left core ($r = 0.36$, $P = 0.010$) connectivity to the right dmPFC.

3.4. Reproducibility and validation analyses

We explored whether the clinically relevant hyperconnectivity patterns showed meaningful accuracy in identifying people with CLBP relative to HCs. We selected all the connections that predicted high pain intensity (positive correlations) after correcting for multiple comparison in the preceding analysis. These comprised 6 NAc-PFC connections as shown in **Figure 5**. We analyzed the effects of using 1 vs 2 resting-state scans, age and sex effects, and spatial intensity smoothing during preprocessing. The validated connections were then analyzed for reproducibility in validation cohorts using statistics and evaluated accuracy using ROC curves.

The distributions and mean rsFC values for the 6 significant contrasts of HC and CLBP for cohort 1 are shown in **Figure 5A**. In addition, the AUC values from ROC analysis for cohort 1 (**Fig. 5B**) showed that the rsFC values between the left shell-right dlPFC, the left core-right dlPFC, left shell-left dmPFCa, and left core-left

dmPFCa were moderate predictors of classifying between HC and CLBP groups (AUC ≥0.7). Because the rsFC observed for CLBP in this analysis was taken from the average of 2 scans, we confirmed that the results remained similar even if the HC rsFC was compared separately for scan 1 and scan 2 (Supplementary Fig. 2, available at http://links.lww.com/PAIN/C271). Owing to the potential concern of spatial smoothing negatively affecting spatial resolution, we also ran the same preprocessing procedure without the 6 mm smoothing filter and confirmed that the results were similar without intensity smoothing for cohort 1 (Supplementary Table 2, available at http://links.lww.com/PAIN/C271). In addition, the rsFC differences between HC and CLBP remained significant after correcting for age and sex (Supplementary Table 3, available at http://links.lww.com/PAIN/C271).

Next, we tested whether these connections could be reproduced in out-of-sample validation data (cohorts 2 and 3 combined) (**Fig. 5C and D**). There was significantly higher connectivity between the left shell with the right dlPFC ($P = 0.003$) and between the left core and right dlPFC ($P = 0.003$) in CLBP relative to HC in this validation set. We also tested the connections for validation cohorts 2 and 3 separately and found that the NAc-dlPFC (right) results reproduced in cohort 2 and trended toward significance in cohort 3 (Supplementary Fig. 3, available at http://links.lww.com/PAIN/C271). The

Table 2

Differences in functional connectivity in the shell and core between chronic low back pain and healthy control subjects after correcting for multiple comparisons.

	Hemisphere	MNI coordinates (x, y, z)	t	P
HC > CLBP (left core)				
Planum polare	L	−48, −4, −6	−4.99	<0.001
Heschls gyrus	L	−48, −18, 6	−4.62	<0.001
Central operculum	L	−48, −4, 8	−4.34	<0.001
Intracalcarine cortex	L	−6, −74, 12	−4.16	<0.001
Middle insula	L	−6, 18, 34	−3.97	<0.001
Hippocampus	L	−28, −22, 16	−3.96	<0.001
Lingual gyrus	L	−10, −68, −2	−3.95	<0.001
Superior temporal gyrus anterior division	L	−58, −4, −6	−3.95	<0.001
Posterior insula	L	−38, −14, 8	−3.89	<0.001
Lingual gyrus	R	10, −68, −2	−3.47	0.001
Intracalcarine cortex	R	−6, −74, 12	−3.28	0.002
Parahippocampal gyrus, posterior division	L	−24, −32, −18	−3.28	0.002
Supracalcarine cortex	L	−2, −84, 12	−3.10	0.003
Planum temporale	L	−60, −22, 8	−2.99	0.004
Temporal occipital fusiform cortex	L	−34, −54, −16	−2.87	0.005
HC > CLBP (left shell)				
Planum polare	L	−48, −4, −6	−5.25	<0.001
Superior temporal gyrus anterior division	L	−58, −4, −6	−4.85	<0.001
Hippocampus	L	−28, −22, −16	−4.55	<0.001
Central operculum	L	−48, 4, 8	−4.35	<0.001
Heschls gyrus	L	−48, −18, 6	−4.33	<0.001
Middle insula	L	−40, −2, −2	−4.06	<0.001
Parahippocampal gyrus, posterior division	L	−24, −32, −18	−4.02	<0.001
Lingual gyrus	L	−10, −68, −2	−3.88	<0.001
Intracalcarine cortex	L	−6, −74, 12	−3.76	<0.001
Posterior insula	L	−38, −14, 8	−3.62	0.001
Temporal occipital fusiform cortex	L	−34, −54, −16	−3.61	0.001
Lingual gyrus	R	10, −68, −2	−3.47	0.001
Superior temporal gyrus, posterior division	L	−66, −26, 6	−3.13	0.002
Temporal pole	L	−40, 16, −30	−3.08	0.003
Temporal occipital fusiform cortex	R	34, −54, −16	−3.01	0.004
Temporal fusiform cortex posterior division	L	−36, −16, −32	−3.00	0.004
Planum temporale	L	−60, −22, 8	−2.90	0.005
Occipital fusiform gyrus	L	−28, −76, −14	−2.81	0.006
Intracalcarine cortex	R	6, −74, 12	−2.76	0.007
Hippocampus	R	28, −22, −16	−2.69	0.009
CLBP > HC (left core)				
Dorsolateral prefrontal cortex	R	40, 20, 44	3.69	<0.001
Dorsal medial prefrontal cortex anterior division	L	−4, 50, 28	3.45	0.001
Dorsolateral prefrontal cortex	L	−40, 20, 44	3.19	0.002
Dorsal medial prefrontal cortex posterior division	L	−4, 26, 48	3.01	0.003
Dorsal medial prefrontal cortex posterior division	R	4, 26, 48	2.97	0.004
Dorsal medial prefrontal cortex anterior division	R	4, 50, 28	2.84	0.006
CLBP > HC (left shell)				
Dorsolateral prefrontal cortex	R	40, 20, 44	3.96	<0.001
Dorsal medial prefrontal cortex anterior division	L	−4, 50, 28	3.41	0.001
Dorsolateral prefrontal cortex	L	−40, 20, 44	3.31	0.001
Dorsal medial prefrontal cortex posterior division	L	−4, 26, 48	3.24	0.002
Dorsal medial prefrontal cortex posterior division	R	4, 26, 48	3.06	0.003
Dorsal medial prefrontal cortex anterior division	R	4, 50, 28	2.92	0.005

Table 2 (*continued*)

	Hemisphere	MNI coordinates (x, y, z)	*t*	*P*
HC > CLBP (right shell)				
Hippocampus	L	−28, −22, −16	−3.92	<0.001
Posterior insula	L	−38, −14, 8	−3.77	<0.001
Central operculum	L	−48, −4, 8	−3.45	0.001
Planum polare	L	−48, −4, −6	−3.45	0.001
Heschls gyrus	L	−48, −18, 6	−3.45	0.001
Superior temporal gyrus, anterior division	L	−58, −4, −6	−3.40	0.001

No significant values were found for the right core, HC > CLBP and CLBP > HC, as well as for right shell, CLBP > HC.
CLBP, chronic low back pain; HC, healthy control.

shorter resting-state scan and lower acquisition resolution may have contributed to nonsignificant results in cohort 3. To study the sensitivity and specificity of the identified functional connectivity patterns in distinguishing CLBP from HC, we used an ROC analysis. None of the connections reached an AUC >0.7 in validation cohorts; however, 2 connections had AUC ≥0.65 (**Fig. 5D**).

3.5. Combined nucleus accumbens-dorsolateral prefrontal cortex resting-state functional connectivity gives higher accuracy for distinguishing healthy control and chronic low back pain groups

The NAc connectivity with right dlPFC showed the most consistent difference between CLBP and HC in the preceding results. Hence, we compared the connectivity of all 4 NAc regions (left and right shell and core) with the right dlPFC in the test and validation groups for their combined accuracy in distinguishing between HC and CLBP groups. The connectivity patterns were consistent: the left and right core, and the right shell showed hyperconnectivity with the right dlPFC in CLBP and individually showed a low-to-moderate accuracy in distinguishing HC from CLBP (**Fig. 6**). Significance for the comparisons was not tested to avoid circular analysis.

Adding all 4 connectivity scores to a logistic regression model for classifying HC vs CLBP using the ENTER method showed a high accuracy for classification. In the test set, 74% cases of CLBP could be accurately classified, where the model explained a moderate portion of variance in rsFC (Nagelkerke R^2 = 0.272) and the −2 Log Likelihood was 92.6, indicating the fit of the model to the data. In the validation set, 83% cases of CLBP could be accurately classified. The model explained a moderate portion of variance in rsFC (Nagelkerke R^2 = 0.38). The −2 Log Likelihood was 122.4 indicating the model fit.

Next, we used the 4 NAc rsFC scores to assess accuracy with a ML-based approach in all available data (cohorts 1, 2, and 3; n = 197, CLBP = 92 and HC = 105). Data were randomised with an 80% training set with 5-fold cross validation and 20% test holdout set. The results comparing 4 different types of classifiers are summarized in **Table 3**. Machine learning–based logistic regression emerged as the best classifier for this data set, demonstrating highest performance in the holdout test set.

Effects of age and sex were tested by pooling data for the identified connections from all 3 cohorts and comparing CLBP with HC by using a MANCOVA. The overall model and all post hoc comparisons between the 2 groups were significant ($P < 0.001$) after correction. There were no significant main interaction effects of age ($P = 0.35$) or sex ($P = 0.77$).

3.6. Exploratory correlation analysis with chronic pain symptoms and demographics

Effects of age and sex were tested by pooling data for the 6 identified connections from all 3 cohorts and comparing the connectivity of CLBP with HC while using age and sex as a covariate (MANCOVA). The overall model and all post hoc comparisons between the 2 groups were significant ($P < 0.001$) after age and sex correction. There were no significant main interaction effects of age ($P = 0.35$) or sex ($P = 0.77$).

To assess the clinical significance and behavioral relevance of the identified connections in cohorts 1 and 2, we summarized the rsFC results by averaging: (1) rsFC values between the right dlPFC and the left core, left shell, and (2) rsFC values between the left and right dmPFCa and each of the 4 NAc regions. We then separately correlated the averaged rsFC values for (1) and (2) with clinical metrics (BPI, Beck Depression Inventory, State-Trait Anxiety Inventory state and trait, MPQ sensory and affective, MQS, Pain Catastrophizing Scale, and Pain Vigilance and Awareness Questionnaire) in the CLBP group. Significant (uncorrected) positive correlations were found between NAc-dlPFC rsFC averages (see 1) and affective MPQ scores ($r = 0.3$, $P = 0.036$, n = 50), higher pain intensity (BPI average pain: $r = 0.22$, $P = 0.029$), and number of areas affected (BPI, $r = 0.192$, $P = 0.048$). In addition, higher NAc-dmPFCa rsFC averages (see 2) were significantly associated with higher BPI current pain intensity ($r = 0.199$, $P = 0.034$) and greater medication use on MQS ($r = 0.196$, $P = 0.042$). No other metrics showed significant associations with the identified rsFC values.

4. Discussion

Both animal and human studies have suggested that hyperconnectivity between the NAc and its prefrontal connections is implicated in the aetiology of CLBP.[6,24,27,30,31,60] We also report NAc-PFC hyperconnectivity in people with CLBP. These connections were predictive of higher CLBP intensity, underscoring their clinical relevance. Of these, only the NAc-right dlPFC connections could be reproduced in new cohorts of participants with different demographics and data acquisition parameters. Combining all 4 NAc-right dlPFC functional connectivity values gave a classification accuracy of 84% in the validation cohort. A ML-based approach in which all data were combined, randomised, and split into test and holdout data sets gave a similar accuracy of 77.5% in the holdout sample. Given the roles of the NAc and dlPFC in reward, motivation, and executive functions, further investigation with larger, more diverse cohorts is needed to uncover mechanistic insights into maladaptive cognitive and motivational responses to CLBP and to confirm CLBP-related neural adaptations.

4.1. Differential nucleus accumbens core and shell connectivity in healthy control and chronic low back pain

The NAc serves as a central hub within the brain's reward circuitry, facilitating motivation processing to acquire rewards and avoid unpleasant stimuli.[40–42] Working alongside sensory regions
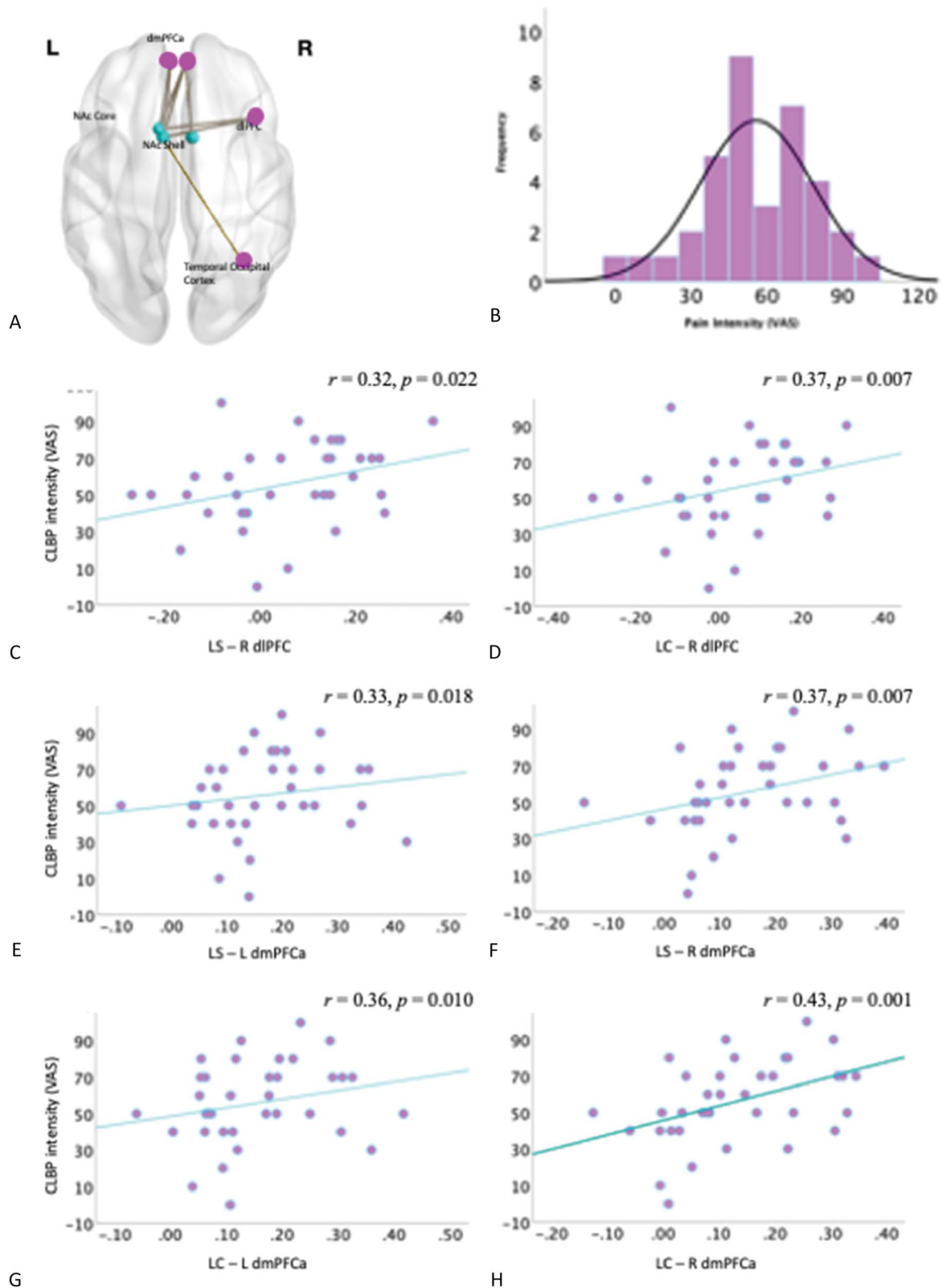
Figure 4. The significant contrasts in the CLBP > HC rsFC comparison were used in further analyses to determine clinical pain parameter correlations. (A) Axial view of significant rsFC connections between the NAc shell and core and regions that were correlated with chronic pain intensity. (B) Distribution of the pain intensity scores. (C-H) Scatter plots of CLBP intensity with the (C) LS-R dlPFC, (D) LC-R dlPFC, (E) LS-L dmPFCa, (F) LS-R dmPFCa, (G) LC-L dmPFCa, and (H) LC-R dmPFCa. LC, left core; LS, left shell; NAc, nucleus accumbens; dmPFCa, dorsal medial prefrontal cortex anterior division; dlPFC, dorsolateral prefrontal cortex; rsFC, resting-state functional connectivity; VAS, visual analog scale. Correlations were false discovery rate corrected for multiple comparisons at $q < 0.1$.
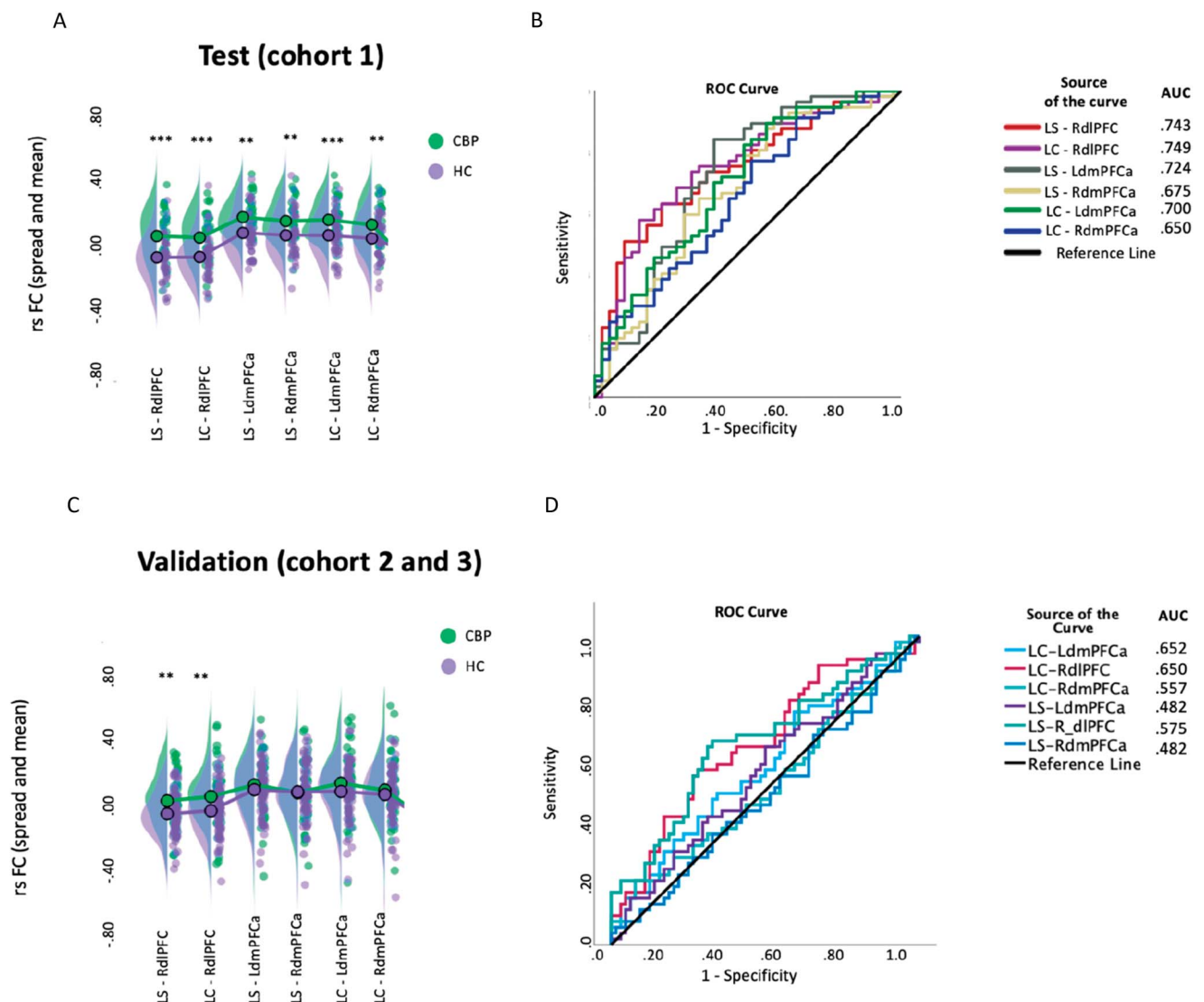
Figure 5. The connections that were significantly correlated with chronic pain intensity were assessed for reproducibility and accuracy for classifying between CLBP and HC groups in the test data set (cohort 1) and in the validation data sets (cohorts 2 and 3). (A) The comparison of connections between HC (n = 41) and the combined CLBP rest 1 and rest 2 groups (n = 39 CLBP) representing the test data set. (B) The ROC curves revealed 4 of 6 connections to be moderate predictors (AUC >0.7) of classifying between HC and CLBP. (C) The validation data set (n = 52 CLBP and 54 HC) showed partly reproducible differences between groups in connections from the left shell and core to the right dlPFC. (D) The ROC curve associated with the validation data set. All HC data and the validation CLBP data were taken from a single resting-state scan (A). AUC, area under ROC curve; dlPFC, dorsolateral prefrontal cortex; dmPFCa, dorsal medial prefrontal cortex anterior division; LC, left core; LS, left shell; ROC, receiver operator characteristic; RS, right shell. Significances: #P = 0.05, *$P < 0.05$, **$P < 0.01$, ***$P < 0.001$.

and the basal ganglia, the NAc controls the impact of sensory input on our behavioral responses. The NAc helps prioritize certain types of actions to achieve goals through its connectivity with the PFC. It adjusts behaviors such as physical effort, reacting to familiar cues, anticipating events, or controlling responses to reach objectives.[39–41] In pathological states such as CLBP or major depressive disorder, disturbances in NAc connectivity can lead to dysregulation in emotional processing and motivational deficits.[4,43,44] We report that the shell of the NAc exhibited greater connectivity with the DMN and regions related to language and memory processing compared with the core in both HC and participants with CLBP. By contrast, the core showed stronger connections with sensory and subcortical regions in both groups. However, in comparisons between HC and CLBP patients, both the shell and core of the NAc were hyperconnected with the PFC and hypoconnected with sensory regions in the CLBP group. This shift suggests that individuals with CLBP may direct more attention toward internal processes, such as managing chronic

pain, rather than external sensory inputs, but this assumption needs to be verified with additional research.

4.2. Nucleus accumbens-prefrontal cortex connectivity in animal models

Our findings indicate that the NAc was hyperconnected exclusively with the PFC. Several of these connections were significantly associated with higher CLBP intensity. The PFC is important for executive functions such as cognitive control, decision-making, and emotion regulation. The NAc facilitates coordination between emotion, cognition, and action through habit formation and procedural memory even in the absence of direct rewards.[9,12,17] In rodent models, dopaminergic NAc-PFC pathways help align behavior with cognitive and emotional states by filtering or amplifying motivational information.[40] These circuits show increased sensitization in neuropathic conditions, which alters behavioral responses to rewards such as morphine.[24] In
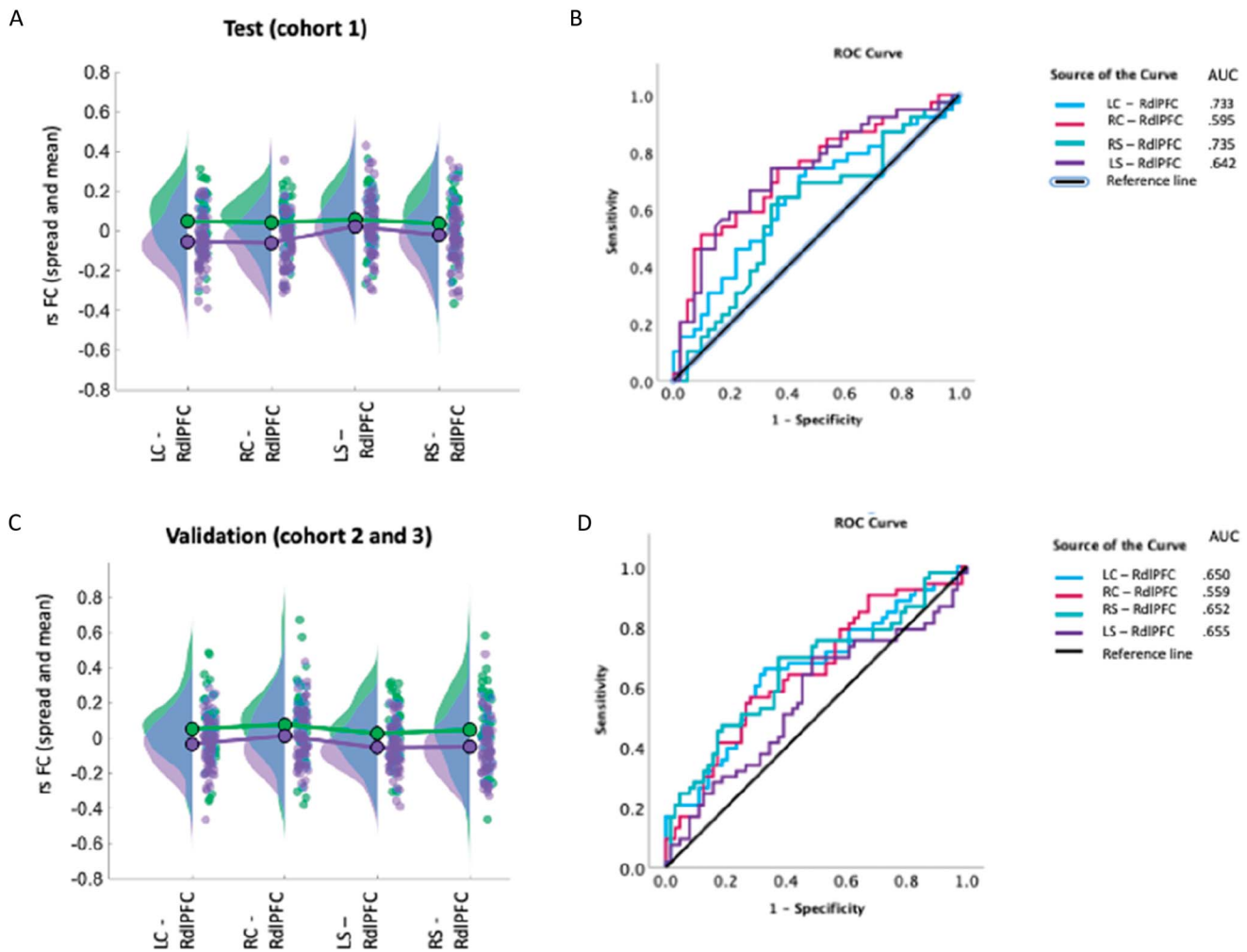
Figure 6. The 4 NAc connections with right dlPFC were assessed for reproducibility and accuracy in classifying between CLBP and HC in the test and validation data sets. (A) Raincloud plot for the comparison of connections between HC (n = 41) and the combined CLBP rest 1 and rest 2 groups (n = 39 CLBP). (B) The ROC curves associated with the test data set (cohort 1). For all 4 connections combined in a logistic regression model, the accuracy was 74%. (C) Raincloud plot for the comparison of groups in the validation data set (cohort 2 and 3, n = 52 CLBP and 54 HC) showed reproducibility of the differences observed in the test data set. (D) The ROC curve associated with the validation data set. For all 4 connections combined in a logistic regression model, the accuracy was 83%. HC data and validation CLBP data were taken from a single resting-state scan (A). AUC, area under ROC curve; dlPFC, dorsolateral prefrontal cortex; LC, left core; RC, right core; LS, left shell; RS, right shell; ROC, receiver operator characteristic.

addition, inhibiting PFC activity or its projections to the NAc increases both sensory and affective components of acute pain in rodent studies.[60] Given the findings in animal models and the results of previous human research, NAc-PFC hyperconnectivity observed in CLBP patients likely reflects changes in motivational and coping mechanisms related to chronic pain.

4.3. Nucleus accumbens-prefrontal cortex hyperconnectivity and chronic low back pain–related dysregulation

In humans, higher connectivity in the NAc-PFC pathway has been shown to predict the development of CLBP from a subacute stage.[6,31] Nucleus accumbens-mPFC connectivity in people with subacute back pain predicts the development of CLBP after 6 months.[6] A recent study validated these earlier findings on the role of NAc-mPFC connectivity, reporting that the process of updating the value of reinforcements (ie, prediction error) in the NAc predicts transition to chronicity.[30] This finding indicates that the prediction error–related uncertainty that ensues from pain contributes to a rewiring of motivational circuitry, resulting in

altered behaviours in pain avoidance and fear of pain. The mPFC, which is crucial for regulating reward-seeking behaviors,[10,56] was shown to activate significantly more in association with fluctuations in back pain in the pain persistence group but not in those that recovered.[21]

In our study, the NAc connectivity with mPFC was not elevated in people with longstanding CLBP, but instead showed hyperconnectivity with the lateral PFC (dlPFC) and the medial PFC (dmPFC). The lateral PFC is implicated in executive functions such as working memory, decision-making, and cognitive control, facilitating goal-directed behavior and managing external information.[1,19] The medial PFC is primarily associated with self-referential processing and the DMN, engaging in tasks involving introspection and personal relevance.[19,28] The dmPFC, in particular, plays a critical role in evaluating potential risks and rewards and selecting appropriate actions based on these evaluations,[15,56] indicating that the NAc may be involved in altered cognitive and motivational processes in CLBP. Notably, the CLBP group showed stronger NAc-dlPFC synchrony, which suggests an increased motivational drive for cognitive and executive functions such as thinking and planning. In other

Table 3

Performance of different classifiers using 5-fold cross-validation and final evaluation on the holdout test set.

Classifier	Train CV accuracy (5-fold), %	Train CV F1 score (5-fold), %	Holdout accuracy, %	Holdout F1 score, %
Logistic regression	58.12	57.40	77.50	77.37
Random forest	51.05	51.70	75.00	74.94
SVM	56.23	55.70	75.00	75.00
KNN	58.06	58.85	70.00	69.31

CV, cross-validation; KNN, k-nearest neighbors; SVM, support vector machine.

conditions such as major depression, decreased NAc-dlPFC connectivity predicts higher depression scores and is associated with substance use disorders.[59] By contrast, NAc-dlPFC hyperconnectivity predicted pain intensity, widespread pain, and greater negative affect related to pain in CLBP patients. In addition, NAc-dmPFCa connectivity predicted higher pain catastrophizing and hypervigilance scores. These psychometric scales are linked with counterproductive avoidance behaviors that lead to disability.[45,47,58] Given the established roles of the NAc and dlPFC/dmPFCa in motivation and cognitive control, these findings suggest that abnormal NAc-PFC connectivity may underlie dysregulated motivation and cognitive processing that become involved with persistent pain in CLBP patients. However, because reward and motivation were not directly tested, any interpretation of the findings based on the described roles of these regions remains speculative.

The NAc-dmPFC also showed significantly increased functional connectivity in CLBP relative to HC, but this finding was more variable between study cohorts. The dlPFC and dmPFC have strong connectivity with each other and work in tandem with the DMN to appraise and regulate emotion.[35,49] For instance, the dlPFC and dmPFC communicate in a sequential manner to resolve cognitive conflict through cross-frequency coupling between gamma and theta oscillations.[51] Another study reported that the dlPFC and dmPFC act as neural hubs to process predictable and unpredictable threats, respectively.[50] Together, these findings indicate that different PFC subregions underpin different stages of CLBP pathophysiology, and that altered PFC synchronizations with the NAc contribute to maladaptive top-down processing in CLBP.[34]

4.4. Reproducibility and methodological considerations

We further report reproducible differences in NAc-PFC connectivity in 3 separate cohorts of participants using a standard statistical approach and a ML-based approach. To test generalizability, each cohort had different demographic parameters. One offsite cohort also had different acquisition and data resolution parameters. Nucleus accumbens functional connectivity was evaluated using atlas-based connectomics and mainly with high temporal resolution fMRI data. We focused on assessing the reproducibility of the connections that were associated with clinical pain intensity after multiple comparison corrections. We aimed to resolve study limitations, including a check to assess whether the smoothing procedure used during preprocessing reduced spatial resolution, thus making it difficult to observe differences between shell and core connectivity (Supplementary Table 2, available at http://links.lww.com/PAIN/C271). We also used stringent motion correction procedures to counter artifacts (see Methods). Because cohort 1 consisted of CLBP data averaged from 2 scans, we also verified comparisons of each resting-state scan acquired in CLBP participants

separately and observed reproducible results (Supplementary Fig. 2, available at http://links.lww.com/PAIN/C271). These analyses indicated that the main findings were reproducible between the 2 scans acquired with the same participants on 2 separate days and hence were not state-dependent. However, we acknowledge that across validation cohorts, the AUC values were weak (<0.7; **Figs. 5 and 6**), suggesting limited discriminative power of individual features across cohorts. Another limitation was significant age differences in the first cohort. To remedy this, we used age and sex corrections (Supplementary Table 3, available at http://links.lww.com/PAIN/C271) and checked the reproducibility of the main findings in additional age- and sex-matched data sets.

We believe our methods will be useful for developing improved schemas on using statistical analyses to select knowledge-based features for ML. By using existing evidence from classical studies, we aim to improve these strategies and generate ML classifiers that are based on mechanistic evidence and agent-based predictors. Such domain knowledge-based predictors will lead to ML-based classifiers that are informed by scientific evidence, hypotheses, and statistical validation.

4.5. Implications and future directions

The concordance between our findings and studies on the transition from acute to chronic back pain further verify that the PFC network is abnormally synchronised with the NAc in CLBP. However, the reliability of these findings depends on the stage of chronic pain, demographics, and data quality. Our study triangulates results from different cohorts to indicate that aberrant NAc-PFC connectivity underpins longstanding CLBP and plays a role in CLBP exacerbations. Our validation efforts demonstrate that NAc-dlPFC rsFC can be reproduced in different cohorts and should be explored further as a predictor for CLBP.

Conflict of interest statement

The authors have no conflicts of interest to declare.   AU2

manuscript preparation. M. A. Hashmi contributed to analyses, tools, and writing the manuscript. J. W. Robertson and J. Veinot contributed to data collection and edits on the manuscript. J. A. Hashmi contributed to analyses, plotting, interpretation, writing, editing the manuscript, and trainee supervision.

Data availability statement: Data will be made available on reasonable request.

Supplemental digital content

Supplemental digital content associated with this article can be found online at http://links.lww.com/PAIN/C271.

AU3 ## References

[1] Aly M, Turk-Browne NB. Attention stabilizes representations in the human Hippocampus. Cereb Cortex 2016;26:783–96.
[2] Apkarian AV, Bushnell MC, Treede RD, Zubieta JK. Human brain mechanisms of pain perception and regulation in health and disease. Eur J Pain 2005;9:463–84.
[3] Aristi G, O'Grady C, Bowen C, Beyea S, Lazar SW, Hashmi JA. Top-down threat bias in pain perception is predicted by intrinsic structural and functional connections of the brain. Neuroimage 2022;258:119349.
[4] Baliki MN, Chialvo DR, Geha PY, Levy RM, Harden RN, Parrish TB, Apkarian AV. Chronic pain and the emotional brain: specific brain activity associated with spontaneous fluctuations of intensity of chronic back pain. J Neurosci 2006;26:12165–73.
[5] Baliki MN, Mansour A, Baria AT, Huang L, Berger SE, Fields HL, Apkarian AV. Parceling human accumbens into putative core and shell dissociates encoding of values for reward and pain. J Neurosci 2013;33:16383–93.
[6] Baliki MN, Petre B, Torbey S, Herrmann KM, Huang L, Schnitzer TJ, Fields HL, Apkarian AV. Corticostriatal functional connectivity predicts transition to chronic back pain. Nat Neurosci 2012;15:1117–9.
[7] Beck AT, Steer RA, Ball R, Ranieri WF. Comparison of Beck Depression Inventories-IA and-II in psychiatric outpatients. J Personal Assess 1996; 67:588–97.
[8] Biswal BB, Mennes M, Zuo XN, Gohel S, Kelly C, Smith SM, Beckmann CF, Adelstein JS, Buckner RL, Colcombe S, Dogonowski AM, Ernst M, Fair D, Hampson M, Hoptman MJ, Hyde JS, Kiviniemi VJ, Kötter R, Li SJ, Lin CP, Lowe MJ, Mackay C, Madden DJ, Madsen KH, Margulies DS, Mayberg HS, McMahon K, Monk CS, Mostofsky SH, Nagel BJ, Pekar JJ, Peltier SJ, Petersen SE, Riedl V, Rombouts SARB, Rypma B, Schlaggar BL, Schmidt S, Seidler RD, Siegle GJ, Sorg C, Teng GJ, Veijola J, Villringer A, Walter M, Wang L, Weng XC, Whitfield-Gabrieli S, Williamson P, Windischberger C, Zang YF, Zhang HY, Castellanos FX, Milham MP. Toward discovery science of human brain function. Proc Natl Acad Sci U S A 2010;107:4734–9.
[9] Block AE, Dhanji H, Thompson-Tardif SF, Floresco SB. Thalamic–prefrontal cortical–ventral striatal circuitry mediates dissociable components of strategy set shifting. Cereb Cortex 2007;17:1625–36.
[10] Capuzzo G, Floresco SB. Prelimbic and infralimbic prefrontal regulation of active and inhibitory avoidance and reward-seeking. J Neurosci 2020;40: 4773–87.
[11] Cartmell SCD, Tian Q, Thio BJ, Leuze C, Ye L, Williams NR, Yang G, Ben-Dor G, Deisseroth K, Grill WM, McNab JA, Halpern CH. Multimodal characterization of the human nucleus accumbens. Neuroimage 2019; 198:137–49.
[12] Christakou A, Robbins TW, Everitt BJ. Prefrontal cortical–ventral striatal interactions involved in affective modulation of attentional performance: implications for corticostriatal circuit function. J Neurosci 2004;24: 773–80.
[13] Cleeland CS. Measurement of pain by subjective report. Adv Pain Res Ther 1989;12:391–403.
[14] Cox RW. AFNI: what a long strange trip it's been. Neuroimage 2012;62: 743–7.
[15] Euston DR, Gruber AJ, McNaughton BL. The role of medial prefrontal cortex in memory and decision making. Neuron 2012;76:1057–70.
[16] Fischl B. FreeSurfer. Neuroimage 2012;62:774–81.
[17] Floresco SB. The nucleus accumbens: an interface between cognition, emotion, and action. Annu Rev Psychol 2015;66:25–52.
[18] Galer BS, Jensen MP. Development and preliminary validation of a pain measure specific to neuropathic pain: the Neuropathic Pain Scale. Neurology 1997;48:332–8.
[19] Gilbert SJ, Gonen-Yaacovi G, Benoit RG, Volle E, Burgess PW. Distinct functional connectivity associated with lateral versus medial rostral prefrontal cortex: a meta-analysis. Neuroimage 2010;53:1359–67.
[20] Harden RN, Weinland SR, Remble TA, Houle TT, Colio S, Steedman S, Kee WG; American Pain Society Physicians. Medication Quantification Scale Version III: update in medication classes and revised detriment weights by survey of American Pain Society Physicians. J Pain 2005;6: 364–71.
[21] Hashmi JA, Baliki MN, Huang L, Baria AT, Torbey S, Hermann KM, Schnitzer TJ, Apkarian AV. Shape shifting pain: chronification of back pain shifts brain representation from nociceptive to emotional circuits. Brain 2013;136:2751–68.
[22] Hashmi JA, Loggia ML, Khan S, Gao L, Kim J, Napadow V, Brown EN, Akeju O. Dexmedetomidine disrupts the local and global efficiencies of large-scale brain networks. Anesthesiology 2017;126:419–30.
[23] Jenkinson M, Beckmann CF, Behrens TEJ, Woolrich MW, Smith SM. Fsl. Neuroimage 2012;62:782–90.
[24] Kai Y, Li Y, Sun T, Yin W, Mao Y, Li J, Xie W, Chen S, Wang L, Li J, Zhang Z, Tao W. A medial prefrontal cortex-nucleus acumens corticotropin-releasing factor circuitry for neuropathic pain-increased susceptibility to opioid reward. Transl Psychiatry 2018;8:100.
[25] Khan S, Hashmi JA, Mamashli F, Hämäläinen MS, Kenet T. Functional significance of human resting-state networks hubs identified using MEG during the transition from childhood to adulthood. Front Neurol 2022;13: 814940.
[26] Kuner R, Kuner T. Cellular circuits in the brain and their modulation in acute and chronic pain. Physiol Rev 2021;101:213–58.
[27] Lee M, Manders TR, Eberle SE, Su C, D'amour J, Yang R, Lin HY, Deisseroth K, Froemke RC, Wang J. Activation of corticostriatal circuitry relieves chronic neuropathic pain. J Neurosci 2015;35:5247–59.
[28] Lee S, Williams ZM. Role of prefrontal cortex circuitry in maintaining social homeostasis. Biol Psychiatry 2024. doi:10.1016/j.biopsych.2024.07.007 **AU4**
[29] Lim M, O'Grady C, Cane D, Goyal A, Lynch M, Beyea S, Hashmi JA. Threat prediction from schemas as a source of bias in pain perception. J Neurosci 2020;40:1538–48.
[30] Löffler M, Levine SM, Usai K, Desch S, Kandić M, Nees F, Flor H. Corticostriatal circuits in the transition to chronic back pain: the predictive role of reward learning. Cell Rep Med 2022;3:100677.
[31] Makary MM, Polosecki P, Cecchi GA, DeAraujo IE, Barron DS, Constable TR, Whang PG, Thomas DA, Mowafi H, Small DM, Geha P. Loss of nucleus accumbens low-frequency fluctuations is a signature of chronic pain. Proc Natl Acad Sci U S A 2020;117:10015–23.
[32] McCracken LM. "Attention" to pain in persons with chronic pain: a behavioral approach. Behav Ther 1997;28:271–84.
[33] Melzack R. The short-form McGill pain questionnaire. PAIN 1987;30: 191–7.
[34] Nees F, Ruttorf M, Fuchs X, Rance M, Beyer N. Brain-behaviour correlates of habitual motivation in chronic back pain. Sci Rep 2020;10: 11090.
[35] O'Reilly RC. The what and How of prefrontal cortical organization. Trends Neurosci 2010;33:355–61.
[36] Pak V, Hashmi JA. Top-down threat bias in pain perception is predicted by higher segregation between resting-state networks. Netw Neurosci 2023;7:1248–65.
[37] Power JD, Barnes KA, Snyder AZ, Schlaggar BL, Petersen SE. Spurious but systematic correlations in functional connectivity MRI networks arise from subject motion. Neuroimage 2012;59:2142–54.
[38] Saghayi M, Greenberg J, O'Grady C, Varno F, Hashmi MA, Bracken B, Matwin S, Lazar SW, Hashmi JA. Brain network topology predicts participant adherence to mental training programs. Netw Neurosci 2020; 4:528–55.
[39] Salamone JD, Correa M. Motivational views of reinforcement: implications for understanding the behavioral functions of nucleus accumbens dopamine. Behav Brain Res 2002;137:3–25.
[40] Salamone JD, Correa M. The mysterious motivational functions of mesolimbic dopamine. Neuron 2012;76:470–85.
[41] Salamone JD, Correa M, Farrar A, Mingote SM. Effort-related functions of nucleus accumbens dopamine and associated forebrain circuits. Psychopharmacology 2007;191:461–82.
[42] Salamone JD, Wisniecki A, Carlson BB, Correa M. Nucleus accumbens dopamine depletions make animals highly sensitive to high fixed ratio requirements but do not impair primary food reinforcement. Neuroscience 2001;105:863–70.

[43] Schwartz N, Temkin P, Jurado S, Lim BK, Heifets BD, Polepalli JS, Malenka RC. Chronic pain. Decreased motivation during chronic pain requires long-term depression in the nucleus accumbens. Science 2014;345:535–42.

[44] Serafini RA, Pryce KD, Zachariou V. The mesolimbic dopamine system in chronic pain and associated affective comorbidities. Biol Psychiatry 2020;87:64–73.

[45] Sullivan MJL, Bishop SR, Pivik J. The Pain Catastrophizing Scale: development and validation. Psychol Assess 1995;7:524–32.

[46] Vachon-Presseau E, Tétreault P, Petre B, Huang L, Berger SE, Torbey S, Baria AT, Mansour AR, Hashmi JA, Griffith JW, Comasco E, Schnitzer TJ, Baliki MN, Apkarian AV. Corticolimbic anatomical characteristics predetermine risk for chronic pain. Brain 2016;139:1958–70.

[47] Vlaeyen JWS, Crombez G, Linton SJ. The fear-avoidance model of pain. PAIN 2016;157:1588–9.

[48] Wang S, Veinot J, Goyal A, Khatibi A, Lazar SW, Hashmi JA. Distinct networks of periaqueductal gray columns in pain and threat processing. Neuroimage 2022;250:118936.

[49] Wei SY, Chao HT, Tu CH, Li WC, Low I, Chuang CY, Chen LF, Hsieh JC. Changes in functional connectivity of pain modulatory systems in women with primary dysmenorrhea. PAIN 2016;157:92–102.

[50] Wheelock MD, Sreenivasan KR, Wood KH, Ver Hoef LW, Deshpande G, Knight DC. Threat-related learning relies on distinct dorsal prefrontal cortex network connectivity. Neuroimage 2014;102:904–12.

[51] Widge AS, Heilbronner SR, Hayden BY. Prefrontal cortex and cognitive control: new insights from human electrophysiology. F1000Res 2019;8: F1000 Faculty Rev-1696.

[52] Xia M, Wang J, He Y. BrainNet viewer: a network visualization tool for human brain connectomics. PLoS One 2013;8:e68910.

[53] Xia S, Yu J, Huang X, Sesack SR, Huang YH, Schlüter OM, Cao JL, Dong Y. Cortical and thalamic interaction with amygdala-to-accumbens synapses. J Neurosci 2020;40:7119–32.

[54] Xia X, Fan L, Cheng C, Eickhoff SB, Chen J, Li H, Jiang T. Multimodal connectivity-based parcellation reveals a shell-core dichotomy of the human nucleus accumbens. Hum Brain Mapp 2017;38: 3878–98.

[55] Xu Y, Goodacre R. On splitting training and validation set: a comparative study of cross-validation, bootstrap and systematic sampling for estimating the generalization performance of supervised learning. J Anal Test 2018;2:249–62.

[56] Xue G, Lu Z, Levin IP, Weller JA, Li X, Bechara A. Functional dissociations of risk and reward processing in the medial prefrontal cortex. Cereb Cortex 2009;19:1019–27.

[57] Yan H, Shlobin NA, Jung Y, Zhang KK, Warsi N, Kulkarni AV, Ibrahim GM. Nucleus accumbens: a systematic review of neural circuitry and clinical studies in healthy and pathological states. J Neurosurg 2023;138: 337–46.

[58] Zale EL, Ditre JW. Pain-related fear, disability, and the fear-avoidance model of chronic pain. Curr Opin Psychol 2015;5:24–30.

[59] Zhou B, Chen Y, Zheng R, Jiang Y, Li S, Wei Y, Zhang M, Gao X, Wen B, Han S, Cheng J. Alterations of static and dynamic functional connectivity of the nucleus accumbens in patients with major depressive disorder. Front Psychiatry 2022;13:877417.

[60] Zhou H, Martinez E, Lin HH, Yang R, Dale JA, Liu K, Huang D, Wang J. Inhibition of the prefrontal projection to the nucleus accumbens enhances pain sensitivity and affect. Front Cell Neurosci 2018;12: 240.

000 **The nucleus accumbens-prefrontal connectivity as a predictor of chronic low back pain**

Chronic low back pain is associated with hyperconnectivity between the nucleus accumbens and prefrontal cortex, a pattern that predicts pain intensity and was partly reproduced between different study cohorts.

Adam Sunavsky, Muhammad Ali Hashmi, Jason William Robertson, Jennika Veinot, Javeria Ali Hashmi